

This is a repository copy of *Comparison of high power red-emitting diode laser designs for medical applications*.

White Rose Research Online URL for this paper:

<https://eprints.whiterose.ac.uk/222274/>

Version: Published Version

Article:

Ryvkin, B.S. and Avrutin, Evgeny orcid.org/0000-0001-5488-3222 (2024) Comparison of high power red-emitting diode laser designs for medical applications. *Optical and quantum electronics*. 993. ISSN 0306-8919

<https://doi.org/10.1007/s11082-024-06818-5>

Reuse

This article is distributed under the terms of the Creative Commons Attribution (CC BY) licence. This licence allows you to distribute, remix, tweak, and build upon the work, even commercially, as long as you credit the authors for the original work. More information and the full terms of the licence here:

<https://creativecommons.org/licenses/>

Takedown

If you consider content in White Rose Research Online to be in breach of UK law, please notify us by emailing eprints@whiterose.ac.uk including the URL of the record and the reason for the withdrawal request.



Comparison of high power red-emitting diode laser designs for medical applications

Boris Ryvkin¹ · Eugene Avrutin²

Received: 6 January 2024 / Accepted: 8 March 2024 / Published online: 26 April 2024
© The Author(s) 2024

Abstract

A comparison is made between, on the one hand, the red-emitting laser structure currently widely used for medical applications and based on an ultranarrow waveguide layer with a compressively strained QW active layer in it and, on the other hand, the red emitting laser using a broadened asymmetric waveguide structure with a bulk active layer near the *p*-cladding, proposed by us. It is shown that the proposed design promises substantial improvements over the ultranarrow one including lower series and thermal resistances, and higher catastrophic degradation threshold, while maintaining relatively narrow far field and allowing the typical power required for medical applications to be achieved at lower currents, particularly at elevated temperatures.

keywords Semiconductor lasers · Lasers for medicine · Red emitting lasers · AlGaInP · Ultranarrow waveguide · Asymmetric waveguide

1 Background and general considerations

Red-emitting diode lasers find increasingly broad use in medicine (see Hagimoto et al. (2023) and references in it). Ref. Hagimoto et al. (2023) presents some recent results of experimental investigations of broad stripe (80 μm) AlGaInP based lasers emitting in the wavelength range of 630–690 nm for medical applications.

The active layer of a laser of the design of Hagimoto et al. (2023) includes a strained QW and two barriers, which form an ultra-narrow waveguide layer first described in Dumke (1975), Casey and Panish (1978). The use of such ultra-narrow waveguides, in principle, allows the laser to emit only a single transverse mode, with a narrow far field possible (Dumke 1975; Casey and Panish 1978; Boucher and Callahan 2011; Marmalyuk et al. 2017; Shashkin et al. 2020).

The experimentally realised lasers presented in Hagimoto et al. (2023) (especially the lasers emitting at wavelengths greater than 650 nm, for which compressively strained QWs are used) demonstrate very high efficiency at moderate injection current densities.

✉ Eugene Avrutin
eugene.avrutin@york.ac.uk

¹ A F Ioffe Physico-Technical Institute, St. Petersburg, Russia

² School of Physics, Engineering, and Technology, University of York, York, UK

However, with increasing injection current density, the optical power becomes saturated, which is known to be due to strong ohmic heating of the laser and the leakage of electrons into the p -cladding caused by this heating (Bour et al. 1993; Smowton et al. 2002).

Note also that the half-width of the far field for all lasers presented in Hagimoto et al. (2023) was $\approx 31^\circ$, a relatively large value potentially limiting the fibre input efficiency.

In our recent theoretical work (Ryvkin et al. 2020; Avrutin et al. 2021), it was shown that an alternative semiconductor laser design, with an asymmetric large optical cavity waveguide and a bulk active layer near the p -cladding, can yield very efficient lasers, reliably emitting in a single transverse mode and operating in different wavelength ranges. Experiments have confirmed their effectiveness for the eye-safe spectral range (Halman et al. 2019, 2021). As shown in our most recent theoretical papers concerning specifically *red-emitting* lasers (Avrutin and Ryvkin 2022; Ryvkin and Avrutin 2023), optical losses and leakage of electrons from the relatively thin (500–700 Å) active layer into the emitter in the proposed design are greatly suppressed for a given temperature (> 300 K).

The proposed lasers may be useful for medical purposes which require red radiation with a wavelength $\lambda > 650$ nm which penetrates relatively deeply into the skin (Oda 2024). For photodynamic therapy, photosensitizers with absorption maxima in the spectral region $\lambda > 650$ nm are used (Oda 2024), for example, Foscan ($\lambda = 652$ nm) and Photochlor ($\lambda = 660$ nm) (Parab et al. 2023). By varying the operating temperature, both these wavelengths can in principle be accessed by *the same laser*. The elevated-temperature use of any laser is however restricted by the well-known decrease in the laser emission power with temperature, which is due to at least two mechanisms: the increase in the threshold current with temperature (mainly because of the decrease of gain with temperature at a given carrier density), and the decrease in the injection efficiency due to thermal electron escape from the active layer into the p -cladding (which is particularly important in red AlGaInP lasers (Bour et al. 1993; Smowton et al. 2002)). To minimise the latter effect, and generally to increase the efficiency of laser operation, it is desirable to achieve lasing at a value of carrier density in the AL as low as possible. This can be achieved by using a relatively thick active layer with a high confinement factor Γ_a , which can be illustrated using the simple linear approximation $g(N) \approx \sigma_g(N - N_{tr})$ for the dependence of material gain g on carrier density N , with $\sigma_g = \left. \frac{dg}{dN} \right|_{N=N_{tr}}$ and N_{tr} the gain cross-section and transparency carrier densities respectively (the approximation is known to be reasonably accurate for bulk materials, and is acceptable for QWs near transparency). Then, the threshold carrier density for a laser with total cavity loss of α_c is estimated as $N_{th} \approx N_{tr} + \frac{\alpha_c}{\Gamma_a \sigma_g}$. The constant

$\sigma_g = \left. \frac{dg}{dN} \right|_{N=N_{tr}}$ can be expected to be a few times higher in compressively strained QWs used in high-power lasers than in bulk materials which can form the thick AL (Coldren et al. 2012); however this inequality can be compensated in the design with a thick AL, as the confinement factor Γ_a can then be made a few times higher than in a Single (and even Double) strained QW ultranarrow waveguide laser. Besides, the value of N_{tr} is known to be substantially lower in a bulk material than in QWs, see e.g. (Coldren et al. 2012), and in a high power laser it is always desirable to make N_{th} close to N_{tr} , minimising the term $\frac{\alpha_c}{\Gamma_a \sigma_g}$.

Thus, a lower N_{th} value can be expected in the asymmetric laser design with a bulk active layer than in a symmetric ultranarrow one with a QW AL (particularly as the simple linear estimate for N_{th} is a conservative one for QWs—the actual value will be higher due to the noticeably sublinear dependence $g(N)$). This means that the electron leakage current into the laser p -cladding, at a given elevated temperature, will be lower in the proposed asymmetric bulk AL design, affecting threshold current density and injection efficiency, as

discussed in Section B below. We will also discuss other potential advantages of this design such as narrower far field, lower series and thermal resistances, and higher catastrophic degradation threshold.

2 Comparative analysis and discussion

A. Near and far fields and related parameters

The waveguide designs and near fields of the reference ultranarrow symmetric structure of Hagimoto et al. (2023), Dumke (1975) and the proposed asymmetric structure of Avrutin and Ryvkin (2022), Ryvkin and Avrutin (2023) are shown in Fig. 1a and b respectively, as are the corresponding near field (modal) intensity profiles. Note that the zero of the x axis in both cases is located at the interface between the waveguide layer and the p -cladding layer.

The waveguide details of the ultranarrow waveguide structure (Fig. 1a), such as the values of the refractive indices of the layers forming the waveguide and their thicknesses, are not to scale and meant for illustration only, since the corresponding data are not given in Hagimoto et al. (2023). Note however that those data are not necessary for subsequent analysis, since for the ultranarrow waveguide design, the near field and hence all the relevant technical parameters can be reconstructed with good accuracy from *just the far field*, which is known (Hagimoto et al. 2023). In practice, all that is required is the angular half width at half maximum of the far field $\theta_{0.5}$ (we used the value 15.5° as in Hagimoto et al. (2023)). Indeed, since both the optical confinement layer and the active layer in an ultranarrow waveguide are much thinner than the size of the mode, the modal amplitude profile (the near field normalized so that $\int \psi_{NF}^2(x)dx = 1$) can be represented as

$$\psi_{NF}(x) \approx \sqrt{p} \exp(-p|x - x_0|) \tag{1}$$

where p is the decrement of field decay in the claddings, and x_0 is the position of the waveguide centre. We have chosen to set the zero of the x -axis at the p -OCL/ p -cladding interface as in Fig. 1 in order to describe naturally the amount of the light penetrating into the p -cladding and reaching the p -contact (see Fig. 3 and the corresponding discussion below for more detail). Then, $x_0 = -\left(\frac{d_a}{2} + d_{p-OCL}\right)$.

In an ultranarrow structure, by definition, $|x_0| \ll \frac{1}{p}$; its value does not affect the far field. The near field shape (1) corresponds to the far field intensity of

$$I_{FF}(\vartheta) = \left(\frac{p^2 \cos \theta}{p^2 + k_0^2 \sin^2 \theta} \right)^2 \tag{2}$$

Here as usual $k_0 = 2\pi/\lambda$ and the far field profile is normalized so that $I_{FF}(0) = 1$.

This allows the value of p , and hence the shape of the near field (1), to be recovered from the width of the far field as

$$p = k_0 \frac{\sin \theta_{0.5}}{\sqrt{\sqrt{2} \cos \theta_{0.5} - 1}} \tag{3}$$

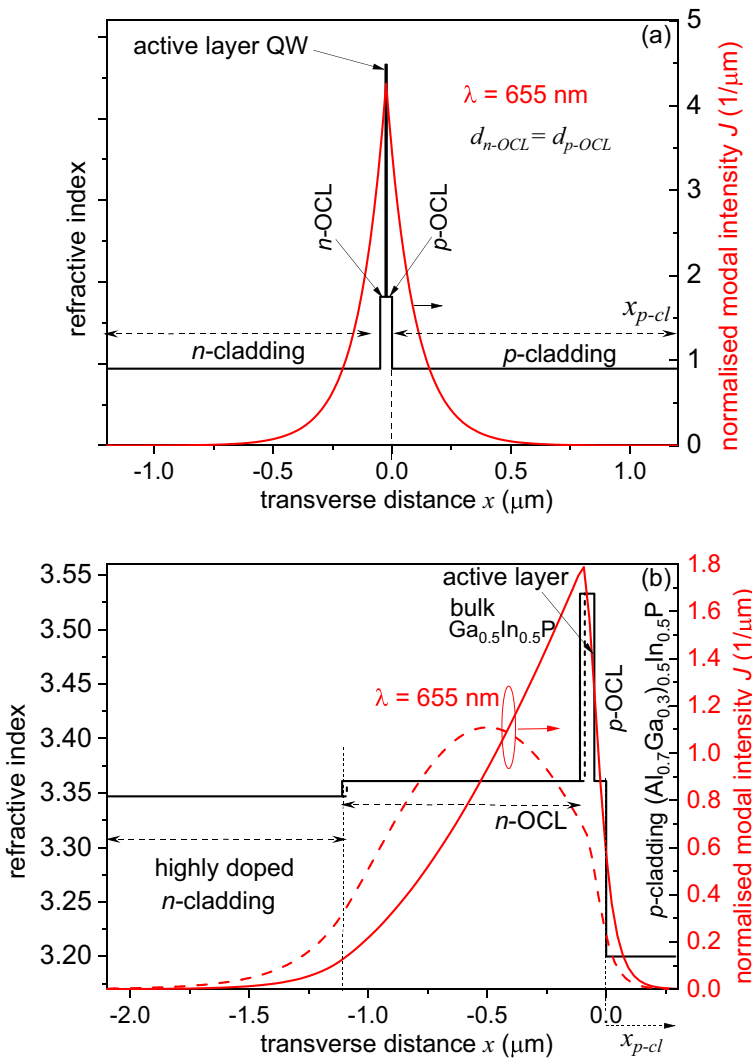


Fig. 1 The waveguide structure and the modal intensity profile of (a) the ultranarrow waveguide laser (waveguide structure schematic; modal profile approximately reconstructed from the far field of (Hagimoto et al. 2023)) and (b) the asymmetric cavity laser as in (Avrutin and Ryvkin 2022; Ryvkin and Avrutin 2023), with the active layer thickness $d_a=0.06 \mu\text{m}$ (solid) and $0.04 \mu\text{m}$ (dashed)

Note that (2) and hence (3) are almost identical to the corresponding formulas given in early sources (Dumke 1975; Casey and Panish 1978), except for the extra factor $\cos^2 \theta$ in (2), and hence $\cos \theta_{0.5}$ in the denominator of (3), which only become important for relatively large values of the transverse angle θ . For $\lambda=0.655 \mu\text{m}$ and $\theta_{0.5}=15.5^\circ$ (Hagimoto et al. 2023) we get $p=4.26 \mu\text{m}^{-1}$, which is used in producing Figs. 1a, 2 and 3.

Figure 2 shows the calculated Far Field profiles for the two laser designs. For the asymmetric cavity laser, we used data from Avrutin and Ryvkin (2022), Ryvkin and Avrutin (2023), with the same active layer thickness values ($d_a=0.04 \mu\text{m}$ and $d_a=0.06 \mu\text{m}$). The far

Fig. 2 Far field profiles for the asymmetric laser design (Avrutin and Ryvkin 2022; Ryvkin and Avrutin 2023) and for the ultranarrow symmetric one

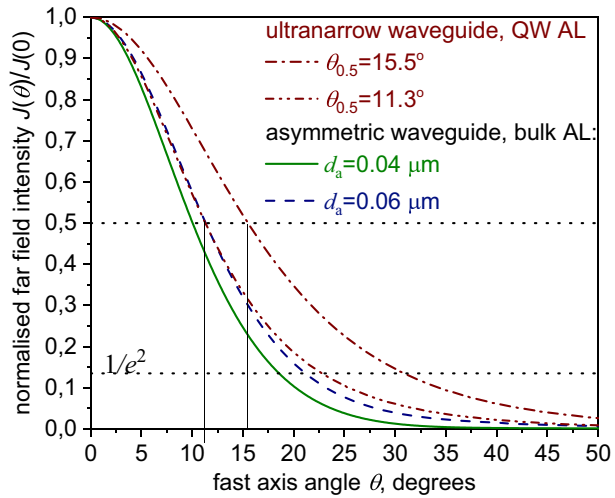
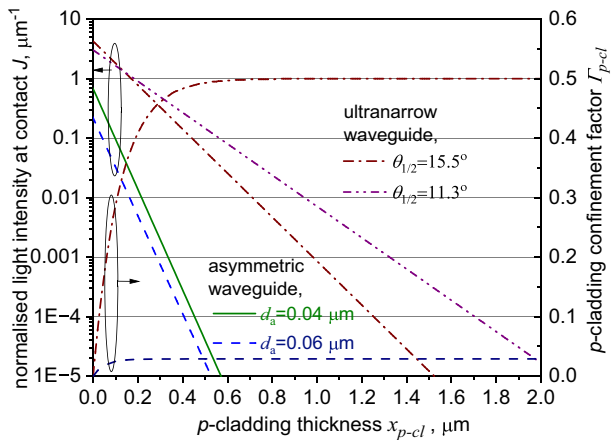


Fig. 3 Dependence of the modal intensity reaching the *p*-contact and the *p*-cladding confinement factor on the *p*-cladding thickness for different laser designs



field profile of the ultranarrow waveguide has been calculated using Eq. (2), with the value of *p* calculated using (3) for two values of $\theta_{0.5}$: firstly, $\theta_{0.5} = 15.5^\circ$ as in Hagimoto et al. (2023) and, secondly, $\theta_{0.5} = 11.3^\circ$ which matches the value predicted for an asymmetric waveguide laser design with $d_a = 0.06 \mu\text{m}$.

As is clearly seen, the proposed asymmetric, bulk active layer laser design is expected to give a substantially narrower far field than that experimentally observed in the ultranarrow waveguide QW AL laser of Hagimoto et al. (2023) (which can be expected for this specific pair of structures given the broader near field in the asymmetric one). By reducing the thickness of the ultranarrow waveguide QW AL laser compared to the one used in Hagimoto et al. (2023), it is possible to match the $\theta_{0.5}$ value of the asymmetric waveguide/bulk AL structure as in Fig. 2, but even in that case, the far field of the asymmetric structure will remain narrower than that of the ultranarrow symmetric one at the $1/e^2$ level.

Figure 3 shows the dependences of normalised modal light intensity profiles $J = \psi^2$ reaching the (lossy) *p*-contact layer (located adjacent to the *p*-cladding, can be seen as the

right extent of Fig. 1), as well as those of the optical confinement factors Γ_{p-cl} , on the p -cladding thickness x_{p-cl} (the distance from the optical confinement layer to the p -GaAs contact layer). With our notations, x_{p-cl} is essentially the extent of the x coordinate in Fig. 1.

The solid and dashed lines in the figure are for the asymmetric waveguide structure of Avrutin and Ryvkin (2022), Ryvkin and Avrutin (2023) as shown in Fig. 1b, and are calculated using the waveguide parameters from Avrutin and Ryvkin (2022), Ryvkin and Avrutin (2023). The dash-dotted lines show the values for the ultranarrow waveguide structure (Fig. 1a) estimated using (1), (3)—the actual Γ_{p-cl} will be slightly lower as some power will be contained within the waveguide layer.

As can be seen from Fig. 3, the value of the modal intensity at the OCL/ p -cladding interface of the ultranarrow waveguide is substantially greater than that for the asymmetric waveguide: $J_{un}(0) \gg J_{as}(0)$. Moreover, the modal intensity of the asymmetric waveguide $J_{as}(x_{p-cl})$ falls with the argument significantly more sharply than the corresponding value for the ultranarrow waveguide $J_{un}(x_{p-cl})$. Thus $J_{un}(x_{p-cl}) \gg J_{as}(x_{p-cl})$, and the difference between them increases exponentially with x_{p-cl} .

The recommended values of the p -cladding thickness for a specific laser design can be estimated from the condition that $J(x_{p-cl})$ does not exceed a certain (very low) value, so that the fraction of radiation absorbed in the p -GaAs contact layer and the metal contact itself (with an absorption coefficient $> 10^4 \text{ cm}^{-1}$) is kept small. Requiring that $J(x_{p-cl}) < 10^{-4}$ gives $x_{p-cl}^{(un)} \sim 1.2 \text{ }\mu\text{m}$ for the reference ultranarrow waveguide and $x_{p-cl}^{(as)} \sim 0.4 \text{ }\mu\text{m}$ for the proposed asymmetric waveguide. Therefore, the series and thermal resistances associated with the p -claddings are much higher in a ultranarrow waveguide laser. Accordingly, asymmetric waveguide bulk active layer lasers promise significantly higher current densities to be accessible without causing significant heating. Earlier, the effect of the p -cladding layer thickness on the performance of AlGaInP lasers was investigated in Smowton et al. (2002). The authors found it very useful to decrease the p -cladding layer thickness in their structure down to $0.5 \text{ }\mu\text{m}$ (further decrease in the emitter thickness led to a sharp increase in optical losses due to absorption in the p -GaAs contact layer). However, in the lasers studied in Smowton et al. (2002), due to noticeable overlap of the optical mode with the highly doped p -cladding layer, free carrier absorption in this layer results in some, non-negligible, optical losses. In our case, the modal overlap with the p -cladding, and hence the free carrier absorption in it, are negligible (Fig. 3). Another design in which the modal overlap with the p -cladding can be made negligible is the Large Optical Cavity AlGaInP laser design with a symmetric relatively thick waveguide (Lichtenstein et al. 2000). This, however, has another limitation since in such a design, the thermal and series resistance improvement is partly limited by the resistance of the lightly doped p -side of the waveguide. In our structure, with the p -side of the waveguide extremely thin, the corresponding resistance is substantially lower. This is very similar to the situation in lasers emitting at a wavelength near $1 \text{ }\mu\text{m}$, with the InGaAs QW active layer located very close to the p -cladding (Crump, et al. 2013; Hasler et al. 2014).

We proceed with comparing the potential of each of the designs from the point of view of reaching the narrow far field without excessive penalty to the active layer confinement factor Γ_a , and hence the threshold carrier density and the threat of carrier leakage. The result is shown in Fig. 4.

We use the far field width as the common technical parameter for the two very different designs. In the proposed design, the variation of the far field width is assumed to be achieved by varying the active layer thickness d_a (Fig. 4a) because in these structures, d_a directly affects waveguiding (Ryvkin et al. 2020; Avrutin et al. 2021; Halman et al. 2019,

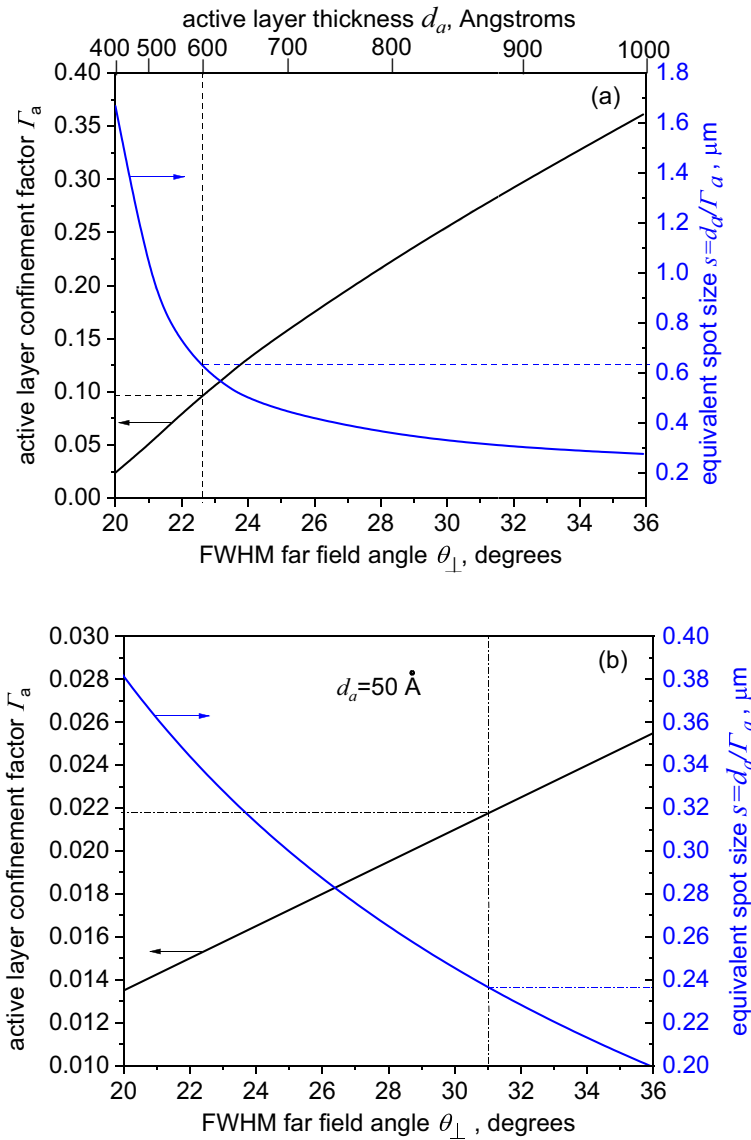


Fig. 4 Active layer confinement factor Γ_a and the equivalent spot size $s = d_a/\Gamma_a$ of the transverse mode for the asymmetric laser design (a) and for the ultranarrow symmetric one (b). Dashed lines indicate the structures with the recommended value $d_a = 600 \text{ \AA}$ and, accordingly, $\theta_{\perp} = 22.6^\circ$ (Fig. 4a) and the experimentally realized (Hagimoto et al. 2023) $\theta_{\perp} = 31^\circ$ (Fig. 4b)

2021). In the reference ultranarrow waveguide, the far field is assumed to be varied by varying the waveguide layer parameters (Shashkin et al. 2020); for example, decreasing θ_{\perp} from the experimental value of 31° (Hagimoto et al. 2023) can be achieved by decreasing the thickness $d_{n-OCL} = d_{p-OCL}$ (Fig. 1a) compared to the value used in Hagimoto et al. (2023) and hence decreasing the field decay decrement p , while keeping the active layer thickness constant at $d_a = 50 \text{ \AA}$ (Kongas et al. 1998; Sumpf et al. 2011). The narrowest far

field represented in the figure corresponds to the p -cladding thickness in the ultranarrow design (necessary to avoid the field reaching the contact layer) of approximately $2\ \mu\text{m}$ —further decrease in θ_{\perp} would have required even broader claddings which we consider impractical from the thermal and series resistance point of view.

As can be expected, in the proposed asymmetric waveguide with its relatively thick bulk active layer, the active layer confinement factor Γ_a is substantially greater than in the reference ultranarrow waveguide—the effect of this difference on the laser performance will be analysed in more detail below (Section B).

Figure 4 also illustrates another important consideration worth noting. An important limitation to the output power of AlGaInP red lasers, such as those compared here, is Catastrophic Optical Degradation (COD) (Lichtenstein et al. 2000). It is well known that COD occurs when the *local optical power density within the active layer* near the facet reaches a certain critical value p_{COD} which can be considered a relatively weak function of the laser structure. The COD power threshold (i.e. the *output* power P_{COD} at which the COD happens) is then evaluated, following (Lichtenstein et al. 2000), as $P_{COD} = p_{COD} \frac{1-R}{1+R} w \frac{d_a}{\Gamma_a}$ (where R is the output facet reflectivity, w the stripe width, d_a the active layer thickness and Γ_a the active layer optical confinement factor) and is thus proportional to the value of the equivalent spot size $s = d_a/\Gamma_a$. This means that in the design proposed in our theoretical papers (Avrutin and Ryvkin 2022; Ryvkin and Avrutin 2023), P_{COD} can be confidently expected to be significantly higher than in the design of Hagimoto et al. (2023)—as can be seen in Fig. 4, this is particularly pronounced for the small values of θ_{\perp} .

This may allow fabrication of lasers without the need for window regions (Hagimoto et al. 2023) or other surface passivation techniques, making for a simpler design, lower fabrication costs and higher yield.

B. Threshold and power characteristics

Knowing the electromagnetic properties of the laser structures (most importantly Γ_a), we can compare the threshold currents as functions of temperature for the asymmetric structure with a bulk active layer and a ultranarrow symmetric waveguide with a compressively strained QW AL (Hagimoto et al. 2023). This characteristic is important, both directly because CW red lasers are operated not too high above threshold so their threshold current has an important effect on the output power, and because it is the main mechanism of the self-heating effect in a CW operated laser and is needed to evaluate the effects of self-heating (though this is not important for the parameter range used here, as discussed below). While with the proposed asymmetric bulk active layer structures, in the absence of experiments, we have to rely on calculated values, for the Quantum Well ultranarrow design we use experimental data as much as possible. Figure 5 shows the temperature dependence $j_{th}(T)$ of the threshold current density for a possible ultranarrow structure operating at $\lambda = 655\ \text{nm}$, obtained by linear interpolation between experimental dependences for $\lambda = 652\ \text{nm}$ and $\lambda = 659\ \text{nm}$ given in Hagimoto et al. (2023) for $T = 303\text{--}323\ \text{K}$ (dashed curve). Shown alongside it is the $j_{th}(T)$ dependence for the proposed asymmetric waveguide, bulk AL design, which has been calculated from first principles using the same model as in the previous papers (Avrutin and Ryvkin 2022; Ryvkin and Avrutin 2023). We have taken the cavity length $L = 1.54\ \text{mm}$ to have approximately the same output losses in both cavities, and for ease of comparison have included on the right vertical axis the full current for a stripe width of $w = 80\ \mu\text{m}$ (note that in Ryvkin and Avrutin (2023), Fig. 6, different values of $w = 200\ \mu\text{m}$ and $L = 2\ \text{mm}$ were assumed).

Fig. 5 Temperature dependence of the threshold current density (left) and the corresponding threshold current for $L = 1.54$ mm, $w = 80$ μm (right) for the ultranarrow design [dashed, interpolated (thicker line) or extrapolated (thin line) from experiment of (Hagimoto et al. 2023) as described in the text], and the proposed asymmetric bulk design (solid, theoretical)

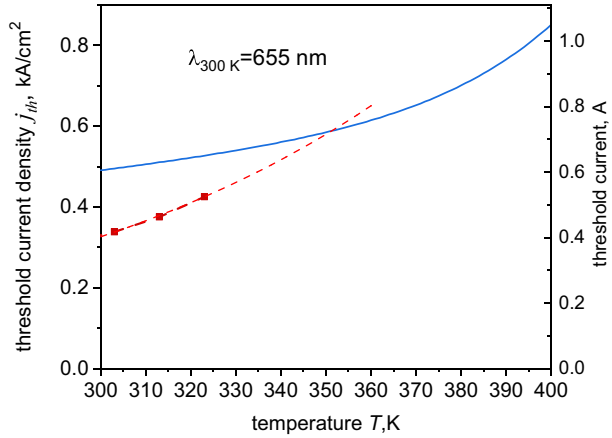
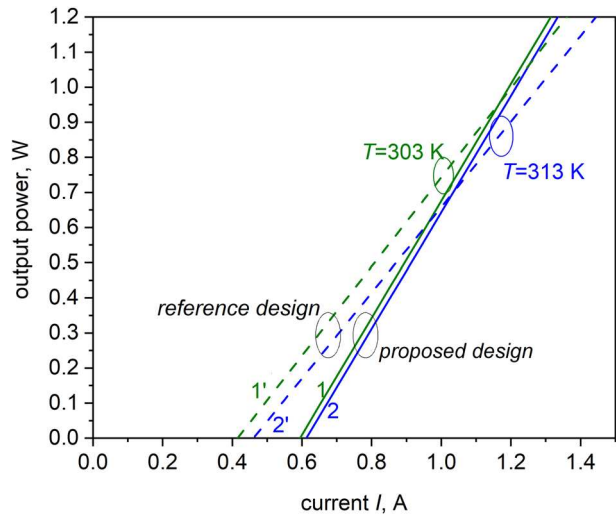


Fig. 6 Light-power curves at temperature of 303 K (1,1') and 313 K (2,2') for the reference ultranarrow design (dashed lines 1',2', extrapolated from the experiment of (Hagimoto et al. 2023) as described in the text), and the proposed asymmetric bulk design (solid lines 1,2, theoretical, $L = 1.54$ mm, $w = 80$ μm as in Fig. 5)



The results show that at room temperature, when the carrier leakage is not very strong, the bulk active layer gives somewhat higher threshold than the QW designs due mainly to the broader AL (note that the d_a value in the proposed laser structure is more than an order of magnitude greater than that in the QW AL for the reference structure, but its j_{th} value is only about 1.5 times greater than in the reference structure, which implies a substantially lower threshold carrier density). The slower threshold increase with temperature (higher characteristic temperature T_0) of the bulk AL (mentioned briefly in Ryvkin and Avrutin (2023)) makes the proposed design advantageous at *elevated* temperatures. Within the experimental temperature range (300–323 K), the dependence $j_{th}(T)$ for the reference (ultranarrow) structure (Hagimoto et al. 2023) is approximated reasonably well by the usual phenomenological relation $j_{th}(T) \approx j_{th}(T_{RT})\exp((T - T_{RT})/T_0)$, with $T_{RT} = 300$ K and $T_0 \approx 87$ K (Fig. 5). Extending the same approximation to higher temperatures (the thin line in Fig. 5), we estimate that the crossover of the two dependences is at no more than 50–55° above room temperature (in practice it can be expected to be lower, as T_0 is known to

decrease with temperature whereas we use a constant room-temperature value). At higher temperatures, the threshold current density of the bulk AL structure is lower than that of the ultranarrow strained-QW one.

From the analysis the threshold current, we can make some predictions on how the output (power) curves) at different temperatures for the two designs will compare with each other. The results are shown in Fig. 6 for two values of temperature: room temperature ($T=303$ K or 30 °C, lines 1,1') and moderately elevated temperature ($T=313$ K or 40 °C, lines 2,2'), for the same cavity geometry as in Fig. 5. The dependences are plotted up to the power of 1.2 W (as in Hagimoto et al. (2023)), which is the typical required power value for a number of medical applications (Hagimoto et al. 2023). For the reference, ultranarrow structure operating at 655 nm, we obtain the light-current curves at 303 K (1') and 313 K (2') in the same way as the data in Fig. 5, by linearly interpolating both the threshold current and the slope efficiency near threshold from the data measured in Hagimoto et al. (2023) for $\lambda=652$ nm and $\lambda=659$ nm. Although the measurements in Hagimoto et al. (2023) were performed under true CW operation, we believe self-heating was negligible, since the light-current dependences are straight lines to a good accuracy for the current/power range and temperatures shown. The dependences for the proposed asymmetric waveguide with a bulk active layer (1, 2) are calculated from first principles as in Ryvkin and Avrutin (2023), taking into account the temperature dependence of the threshold current and injection efficiency. Since we are confident that the thermal resistance of the proposed design can be made no greater than in the reference one (in fact, it is likely to be smaller as discussed above), no self-heating needs to be taken into account in the calculations. Despite the threshold currents of the proposed design being higher than those for the reference one for this range of temperatures, the desired power output of 1.2 W is predicted to be achieved at lower currents for both temperatures, and this current difference increases with temperature. This is due to the high injection efficiency of our lasers which decreases very weakly with temperature under the slight temperature increase above room temperature (Ryvkin and Avrutin 2023).

C. Summary and discussion

Summarising, we note that the proposed lasers are predicted to compare favourably with the state of the art by promising lower series and thermal resistance and higher catastrophic degradation threshold. The lower carrier escape, hence higher injection efficiency, in the proposed laser design leads to a superior power output predicted above a certain injection current level, allowing the required power to be achieved at a lower current, particularly at elevated temperatures. In addition, a narrower far field is predicted, promising more efficient fibre input.

We note finally that the thick AL can, in principle, be either a bulk layer or a Multiple Quantum Well (MQW) one (the wells in it would have to be unstrained, as the number of strained wells in a laser structure is by necessity strongly limited). However the MQW AL with the same *total* thickness as the bulk AL would result in a smaller *active* thickness (excluding the barriers which, in the first approximation, do not contribute to modal gain), and hence $\Gamma_a\sigma_g$ product, compared to a bulk AL. Besides, the relatively large number of QWs that would be required could result in uneven well occupation and also, as mentioned earlier, the value of N_{tr} is lower in a bulk material than in QWs, see e.g. (Coldren et al. 2012). Thus we see no advantages in using a more complex MQW active layer compared

to a bulk one as the regards the modal gain (Avrutin et al. 2020) and have chosen the bulk active layer.

Acknowledgements The authors are grateful to I. Shashkin, the first author of Ref. (Shashkin et al. 2020), for useful discussions.

Author contributions Both authors contributed to analytical and numerical calculations as well as writing the paper.

Funding None.

Data availability Available on request.

Declarations

Conflict of interest None.

Ethical approval Not applicable.

Open Access This article is licensed under a Creative Commons Attribution 4.0 International License, which permits use, sharing, adaptation, distribution and reproduction in any medium or format, as long as you give appropriate credit to the original author(s) and the source, provide a link to the Creative Commons licence, and indicate if changes were made. The images or other third party material in this article are included in the article's Creative Commons licence, unless indicated otherwise in a credit line to the material. If material is not included in the article's Creative Commons licence and your intended use is not permitted by statutory regulation or exceeds the permitted use, you will need to obtain permission directly from the copyright holder. To view a copy of this licence, visit <http://creativecommons.org/licenses/by/4.0/>.

References

- Avrutin, E., Ryvkin, B.: Semiconductor laser design with an asymmetric large optical cavity waveguide and a bulk active layer near p -cladding for efficient high-power red light emission. *Semicond. Sci. Technol.* **37**(12), 125002 (2022)
- Avrutin, E., Ryvkin, B., Kostamovaara, J.: AlGaAs/GaAs asymmetric-waveguide, short cavity laser diode design with a bulk active layer near p -cladding for high pulsed power emission. *IET Optoelectron.* **15**(4), 194–199 (2021)
- Avrutin, E.A., Ryvkin, B.S., Hallman, L.W., Kostamovaara, J.T.: High power 1.5 μm pulsed semiconductor laser design with a bulk active layer and an asymmetric waveguide. In: *Proceedings of 21st International Conference on Transparent Optical Networks (ICTON'2020)*, IEEE, paper TuA5.3, pp. 1–4, (2020)
- Boucher, J.F., Callahan, J.J.: Ultra-high-intensity 1550nm single junction pulsed laser diodes. In: *Proceedings of SPIE 8039*, Orlando, FL, USA, (2011), p. 80390B
- Bour, D.: AlGaInP quantum well lasers. In: Zory, P. (ed.) *Quantum Well Lasers*, pp. 415–460. Academic Press, San Diego (1993)
- Bour, D.P., Treat, D.W., Thornton, R.L., Geels, R.S., Welch, D.F.: Drift leakage current in AlGaInP quantum-well lasers. *IEEE J. Quantum Electron.* **29**(5), 1337–1343 (1993)
- Casey, H., Panish, M.: *Heterostructure Lasers Part A: Fundamental Principles*. Academic Press, New York, San Francisco, London (1978)
- Coldren, L., Corzine, S.W., Masanovic, M.L.: *Diode Lasers and Photonic Integrated Circuits*. Wiley, NY (2012)
- Crump, P., Erbert, G., Wenzel, H., Frevert, C., Schultz, C.M., Hasler, K.-H., Staske, R., Sumpf, B., Maassdorf, A., Bugge, F., Knigge, S., Trankle, G.: Efficient high-power laser diodes. *IEEE J. Select. Topics Quantum Electron.* **19**(4), 1501211–1501211 (2013). <https://doi.org/10.1109/JSTQE.2013.2239961>
- Dumke, W.: The angular beam divergence in double-Heterojunction lasers with very thin active region. *IEEE J. Quantum Electron.* **11**(7), 400–402 (1975)

- Hagimoto, M., Miyamoto, S., Watanabe, K., Hashizume, M., Yano, K.: Red laser diodes explore the future of biomedical and quantum technology. *Proc. SPIE* **12440**, 124400M (2023)
- Halman, L., Ryvkin, B., Avrutin, E., Aho, A., Viheriala, J., Guina, M., Kostamovaara, J.: High power 1.5 μ m pulsed laser diode with asymmetric waveguide and active layer near p-cladding. *IEEE Photon. Technol. Lett.* **31**(20), 1635–1638 (2019)
- Halman, L., Ryvkin, B., Avrutin, E., Kostamovaara, J.: >25 W pulses from 1.5 μ m double-asymmetric waveguide, 100 μ m stripe laser diode with bulk active layer. *Electron. Lett.* **57**(23), 891–893 (2021)
- Hasler, K.H., Wenzel, H., Crump, P., Knigge, S., Maasdorf, A., Platz, R., Staske, R., Erbert, G.: Comparative theoretical and experimental studies of two designs of high-power diode lasers. *Semicond. Sci. Technol.* **29**(4), 045010 (2014). <https://doi.org/10.1088/0268-1242/29/4/045010>
- Kongas, J., Savolainen, P., Toivonen, M., Orsila, S., Corvini, P., Jansen, M., Nabiev, R., Pessa, M.: High efficiency GaInP-AlGaInP ridge waveguide single-mode lasers operation at 650 nm. *IEEE Photon. Technol. Lett.* **10**(11), 1533–1535 (1998) <https://doi.org/10.1109/68.726740>
- Lichtenstein, N., Winterhoff, R., Scholz, F., Schweizer, H., Weiss, S., Hutter, M., Reichl, H.: The impact of LOC structures on 670 nm (Al)GaInP high-power lasers. *IEEE J. Select. Topics Quantum Electron.* **6**(4), 564–570 (2000). <https://doi.org/10.1109/2944.883369>
- Marmalyuk, A.A., Ryaboshtan, Y.L., Gorlachuk, P.V., Ladugin, M.A., Padalitsa, A.A., Slipchenko, S.O., Lyutetskiy, A.V., Veselov, D.A., Pikhtin, N.A.: Semiconductor AlGaInAs/InP lasers with ultra-narrow waveguides. *Quantum Electron.* **47**(3), 272–274 (2017)
- Oda, F.: Biomedical application of deep red color (670–690 nm) laser diodes. (2024) At <https://www.ushio.co.jp/en/laser/news/500888.html> (Accessed 10.02.2024)
- Parab, S., Achalla, P.K., Yanamandala, N., Singhvi, G., Kesharwani, P., Dubey, S.K.: Sensitizers in photodynamic therapy. In: *Nanomaterials for Photodynamic Therapy*, pp. 81–103. Elsevier (2023). <https://doi.org/10.1016/B978-0-323-85595-2.00002-5>
- Ryvkin, B.S., Avrutin, E.A.: Threshold and power of pulsed red-emitting diode lasers with a bulk active layer near p-cladding under high-temperature operation. *Opt. Quantum Electron.* (2023). <https://doi.org/10.1007/s11082-023-04887-6>
- Ryvkin, B., Avrutin, E., Kostamovaara, J.: Asymmetric-waveguide, short cavity designs with a bulk active layer for high pulsed power eye-safe spectral range laser diodes. *Semicond. Sci. Technol.* **35**(8), 085008 (2020)
- Shashkin, I.S., Leshko, A.Y., Nikolaev, D.N., Shamakhov, V.V., Veselov, D.A., Rudova, N.A., Bakhvalov, K.V., Zolotarev, V.V., Slipchenko, S.O., Pikhtin, N.A., Kop'ev, P.: Single-mode lasers (1050 nm) of mesa-stripe design based on an AlGaAs/GaAs heterostructure with an ultra-narrow waveguide. *Semiconductors* **54**(4), 489–494 (2020). <https://doi.org/10.1134/S1063782620040181>
- Smowton, P., Thompson, J., Yin, M., Dewar, S., Blood, P., Bryce, A., Marsh, J., Hamilton, C., Button, C.: The effect of cladding layer thickness on large optical cavity 650-nm lasers. *IEEE J. Quant. Electron.* **38**(3), 285–290 (2002) <https://doi.org/10.1109/3.985570>
- Sumpf, B., Fricke, J., Ressel, P., Zorn, M., Erbert, G., Tränkle, G.: 520 000 h reliable operation of 100 μ m stripe width 650 nm broad area lasers at more than 1.1 W output power. *Semicond. Sci. Technol.* **26**, 105011 (2011)

Publisher's Note Springer Nature remains neutral with regard to jurisdictional claims in published maps and institutional affiliations.